

ESTIMATING RETURN PERIODS OF EXTREME EVENTS FROM ECMWF SEASONAL FORECAST ENSEMBLES

H. W. VAN DEN BRINK,* G. P. KÖNNEN, J. D. OPSTEEGH, G. J. VAN OLDENBORGH and G. BURGERS

Royal Netherlands Meteorological Institute, 3730 AE de Bilt, The Netherlands

Received 14 June 2004

Revised 29 November 2004

Accepted 8 December 2004

ABSTRACT

Meteorological extremes have large impacts on society. The fact that approximately 40% of the Netherlands is below sea level makes this country especially vulnerable to flooding, both from the sea and from rivers. This has resulted in extensive research on the statistics of extremes. However, applications to meteorological and hydrological situations are always hampered by the brevity of the available datasets, as the required return levels exceed the record lengths by a factor of 10 to 100. In order to overcome this problem, we use archived data from all past seasonal forecast ensemble runs of the European Centre for Medium-Range Weather Forecasts (ECMWF) since 1987 as input for extreme-value statistics analysis. We make use of the fact that the seasonal forecast has little seasonal skill for the Netherlands, which implies that the ensembles can be regarded as independent sets that cumulate to over 1500 years.

We investigate the hydraulic response in the Netherlands to extreme synoptic-scale weather systems by studying the extreme-value distributions of sea storm surge levels, waves and river discharges. The application is detailed in four practical examples originating from coastal protection, river flooding protection, and water management problems. The long record length of the ECMWF data reduces the uncertainty in the 10^3 -year and the 10^4 -year return values considerably with respect to the results based on observational time series. The ECMWF dataset gives the opportunity to explore the distribution of events that depend on several kinds of extreme. Copyright © 2005 Royal Meteorological Society.

KEY WORDS: meteorological extremes; surges; river discharges; waves; multivariate extremes; risk analysis; statistical uncertainties

1. INTRODUCTION

Much statistical research has been done on estimating the statistics of extremes of weather (related) variables, like precipitation, wind speed, river discharge and surge from observational records (de Haan, 1990; Buishand, 1991; Palutikof *et al.*, 1999; Katz *et al.*, 2002). To overcome the rather short length of the observational records (order 100 years), we explored an alternative data source, i.e. the archived seasonal forecast ensemble data of the European Centre for Medium-Range Weather Forecasts (ECMWF) over the period 1987–2004, which cumulate to a total size of 1569 simulated years (status May 2004). Assuming that this model is a faithful representation of the climate system, these simulated years represent many realizations of the present climate on a synoptic scale. Because this model dataset is an order of magnitude longer than the length of the observational sets, an improved estimate of extreme levels can be obtained. In an earlier article (van den Brink *et al.*, 2004) we discussed the extreme-value statistics of storm surges at the Dutch coast. We found that the ECMWF model represents the statistics of large and deep depressions well. The statistical uncertainty of the height of a 10^{-4} probability storm surge was decreased by a factor of four compared with the use of the historical observations, with systematic errors that appeared smaller than the statistical uncertainty. As an elaboration of van den Brink *et al.* (2004), in this paper we apply the ECMWF seasonal forecast data set to four hydraulics-related situations in the Netherlands that result from severe weather events on a synoptic

* Correspondence to: H. W. van den Brink, KNMI, PO Box 201, 3730 AE de Bilt, The Netherlands; e-mail: brinkvdh@knmi.nl

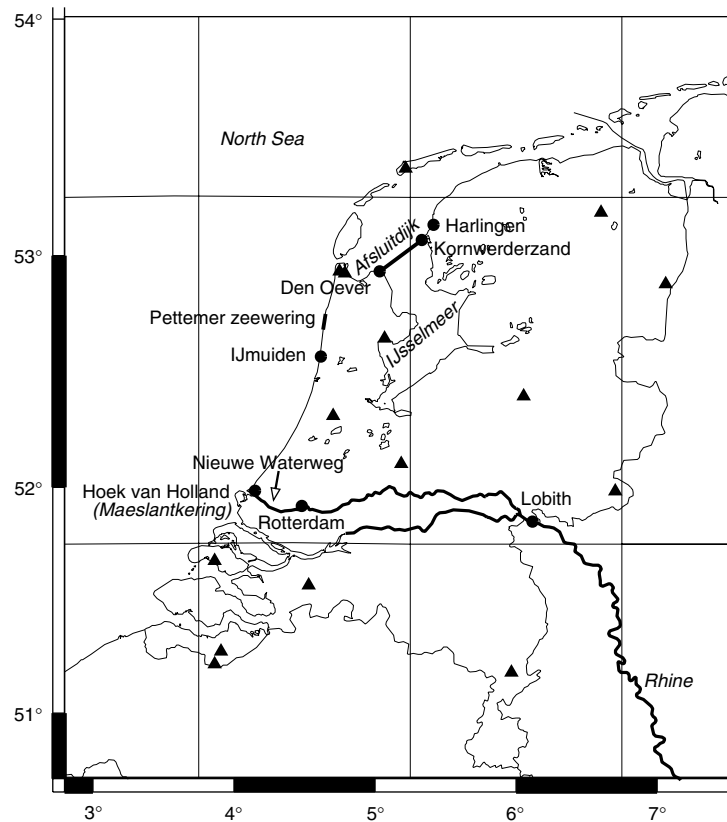


Figure 1. Map of the Netherlands, with the locations that are mentioned in the text. The lines represent the physical grid to which the ECMWF data have been interpolated ($1.5^\circ \times 1.5^\circ$). The triangles are the 15 stations used for verification of the precipitation

scale. First, to extreme Rhine river discharges at the location where it flows into the Netherlands. Second, to the duration of the spells where sea level is too high, sluicing water from the 'IJsselmeer' into the North Sea. Third, to the frequency that the big 'Maeslantkering' storm surge barrier in the 'Nieuwe Waterweg' Rhine outlet must be closed in order to prevent flooding of the densely populated Rotterdam area. The criteria for closing the barrier depend on the sea level and on the Rhine river discharge. Fourth, to the frequency of failure of the 'Pettemer zeewering' sea dike, which depends both on sea level elevation and wave height. See Figure 1 for the locations of the towns, rivers and barriers.

This paper is structured as follows: Section 2 describes the theoretical framework, Section 3 the ECMWF model and seasonal forecast ensembles, Section 4 the extreme-value analysis of the applications mentioned, and Section 5 the conclusions and discussion.

2. THEORY

A fundamental theoretical result from the statistics of extremes is that any limiting distribution of 'block maxima' must be in the form of the generalized extreme value (GEV) distribution (e.g. de Haan, 1976):

$$G(x) = P(M \leq y) = e^{-e^{-x}} \quad (1)$$

with M the maximum over a 'block' of standard length, $G(x)$ the GEV distribution, and x a substitute for

$$x = \ln \left(1 - \theta \frac{y - \mu}{\alpha} \right)^{-1/\theta} \quad (2)$$

with μ the location parameter, α the scale parameter, θ the shape parameter, and y the variable considered. A common choice is to examine the distribution of annual maxima. In this case, the location parameter μ represents the value that is exceeded on average once a year.

In extreme-value studies, the probability of exceedance of a certain value y is usually expressed in terms of the *return period* T , i.e. the average number of years between two succeeding exceedances of the corresponding *return value* y :

$$T = \frac{1}{1 - G(x)} \approx e^x \quad \text{for } T \gg 1 \quad (3)$$

For fitting the data to the GEV distribution, we used the method of maximum likelihood. The 95% confidence values in the return value estimates were determined from the log-likelihood profile (Coles, 2001).

The results are plotted on a Gumbel plot, a plot of a cumulative distribution function $F(x)$ with the Gumbel variate $-\ln[-\ln(F(x))]$ as abscissa and the return value y as ordinate. This representation transforms the Gumbel distribution ($G(x)$ with $\theta = 0$) into a straight line.

Extreme-value theory is often required to find return values for return periods that amply exceed the record length. This implies extrapolation of the GEV fit to a domain outside the range of the observations. In our approach, the return value determination involves little extrapolation, as series length and return periods of interest T are about equal. This considerably reduces the uncertainty in the estimate.

3. ECMWF MODEL

3.1. Description

For September 2001 onward the ECMWF produces every month an ensemble of 40 global seasonal forecasts up to 6 months ahead, i.e. amply surpassing the 2 weeks horizon of weather predictability from the atmospheric initial state. Over the period 1987–2001, hindcasts with smaller ensembles have been performed to calibrate the system. The forecast system consists of a coupled atmosphere–ocean model (Anderson *et al.*, 2003). The atmospheric component has a horizontal resolution of T95 (1.875°) and 40 levels in the vertical (Ritchie *et al.*, 1995; Gregory *et al.*, 2000; Anderson *et al.*, 2003). The ocean component has a resolution of 1.4° and 29 vertical levels (Wolff *et al.*, 1997). We combined all hindcasts and forecasts generated up to May 2004, into 1570 calendar years of data, all of them generated by the so-called System-2 (Anderson *et al.*, 2003). The ECMWF dataset provides, among other fields, global fields of 6 h winds and 2 m temperatures, 12 h sea-level pressures (SLPs) and temperatures, and 24 h precipitation amounts.

3.2. Verification

In order to model hydraulic extreme events correctly, the wind and precipitation in particular should be well represented in the model. As it is difficult to verify the model winds directly (due to the relatively short (homogeneous) observational records over the North Sea), van den Brink *et al.* (2004) validated the SLP instead. This direct model parameter can be compared more easily with observations than wind data, and is a good measure of the capability of the model to produce deep depressions. They found a good agreement between the statistics of extremely low SLPs in the ECMWF model and the observations for coastal station Den Helder. Also, the surge statistics for the coastal station Hoek van Holland are well reproduced by the ECMWF model (van den Brink *et al.*, 2004).

Figure 2 compares the extreme precipitation rates of the mean of the two ECMWF boxes (4.5–6°E, 52.5°N) in the ECMWF data with the accumulated precipitation averaged over 15 stations in the Netherlands (indicated in Figure 1). Both the 1 day and the 20 day accumulated quantities are shown. Figure 2 shows that the statistics of extreme precipitation are well reproduced for both time scales.

In order to investigate the dependence between the ensembles and their initial states, we calculated the correlation between the observed (monthly mean) North Atlantic oscillation (NAO) index and the calculated

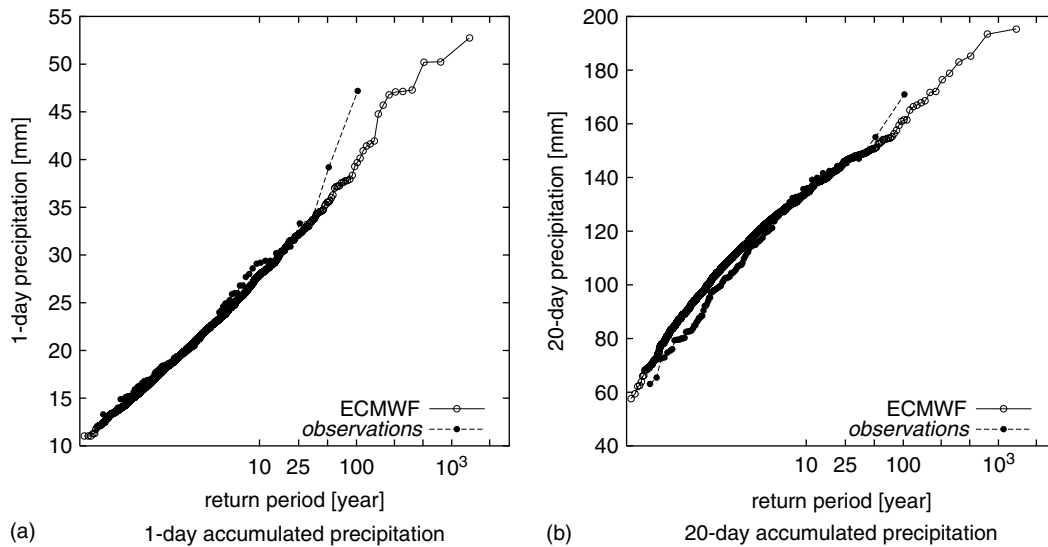


Figure 2. Gumbel plots of (a) the 1 day and (b) 20 day accumulated precipitation, for the average of 15 Dutch stations (1901–2001) and the corresponding ECMWF boxes (4.5–6°E, 52.5°N). See Figure 1 for the locations of the 15 stations

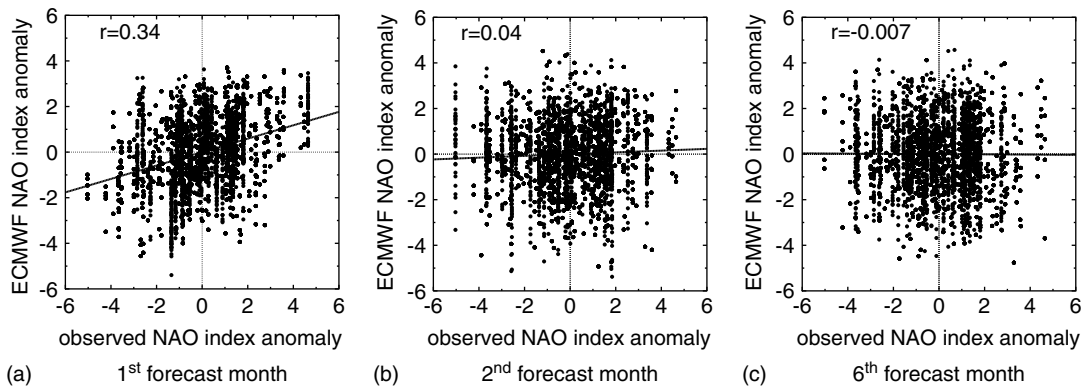


Figure 3. Scatter plot of the NAO index anomaly, (December–March) of the ECMWF seasonal forecast against the observed NAO, for the (a) first (b) second and (c) sixth forecast month. The lines represent a least-squares fit

NAO index from the ECMWF data. Figure 3 shows the scatter plots for different forecast months. For the first forecast month, there is a small correlation ($r = 0.34$) between the monthly averaged NAO of the seasonal forecast and the observed NAO. This correlation is nearly zero ($|r| \leq 0.07$) for longer forecast times. This implies that the NAO index of the ECMWF dataset is (almost) independent of the initial NAO index, and thus is representative for a more general situation than for the 1987–2004 period only. A very similar version of the ECMWF model has also been shown to have very limited skill in predicting the NAO index (Palmer *et al.*, 2004).

The constant variance of the modelled NAO index with the forecast time and the independence of fitted GEV parameters with forecast time indicate that the climatology of the system shows no detectable deterioration with forecast time.

We verified that the dependence between the ensemble members in the first weeks of the forecasts has negligible influence on the estimates of the GEV parameters, making the whole 6 month period usable for our purpose.

4. FOUR APPLICATIONS

4.1. Rhine discharge

The dikes along the Dutch rivers are supposed to withstand a discharge with a return period of 1250 years. The Rhine discharge at the Dutch border and the accumulated n -day precipitation over the Rhine basin correlate well for $n = 10$ –30 (Fink *et al.*, 1996). We concentrate on 20-day accumulated values (validated in Section 3.2).

We calculated the Rhine discharge at Lobith at the Dutch–German border (see Figure 1) with the following simple water balance equation:

$$Q = A + \sum_{j=0}^{19} \sum_i s_i (\text{LSP}_{i,j} + \text{CP}_{i,j} - E_{i,j} - S_{i,j}) \quad (4)$$

with $\text{LSP}_{i,j}$ the large-scale precipitation on the j th-last day in grid box i , of which a surface area s_i (m^2) belongs to the catchment of the Rhine. CP is the convective precipitation, E the evaporation and S the snow accumulation, all in metres of water per second. The adjustment parameter A was determined empirically by tuning the location parameter μ of the GEV distribution (i.e. the once-a-year event) with its observed value at Lobith. A turns out to be $-4 \times 10^3 \text{ m}^3 \text{ s}^{-1}$.

The Gumbel plot of the Rhine discharge according to the observational record at Lobith and to the ECMWF data (Equation (4)) are shown in Figure 4. The estimate from the observations for the 1250 year discharge ($14.3_{12.2}^{20.1} \times 10^3 \text{ m}^3 \text{ s}^{-1}$) is 9% smaller than the estimate from the ECMWF data ($15.7_{14.5}^{17.1} \times 10^3 \text{ m}^3 \text{ s}^{-1}$). The ECMWF estimate lies amply within the 95% uncertainty interval of the estimate from the observations. The application of the ECMWF data reduces the 95% confidence interval of the 1250 year level estimate by a factor three.

4.2. IJsselmeer sluicing

The IJsselmeer (Lake IJssel) in central Netherlands covers an area of 2000 km^2 and is separated from the North Sea by the Afsluitdijk. To keep the level of the IJsselmeer at the preferred level of 0.45 m below mean

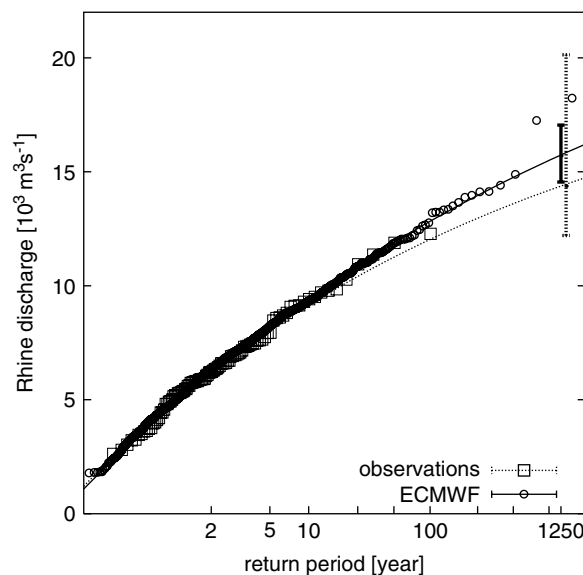


Figure 4. Gumbel plot for the 100 observed annual maximum Rhine discharges at Lobith (1900–2000) (\square) and for the 1569 annual maxima as derived from the ECMWF data via Equation (4) (\circ). Also shown are the extrapolated GEV fits to 1250-year return periods and the 95% confidence intervals to the observations and to the ECMWF data

sea level (MSL) in winter (and 0.25 m below MSL in summer) (Peilbesluit wateren IJsselmeergebied, 1992), the excess of IJsselmeer water is discharged into the North Sea during low tide by opening the Afsluitdijk sluices at Kornwerderzand and Den Oever (low lower tide at Kornwerderzand: 1.23 m below MSL). During high tide, the sluice gates are closed. If a surge elevates the low-tide sea level above a value of 0.55 m below MSL, then sluicing is not possible during an entire tidal cycle.

To examine the period that surges prevent sluicing, we calculated the sea level at every low tide by adding the surge to the astronomical low tide, where the 6 h calculated surge was linearly interpolated to the time of the astronomical low tide. The harmonical constituents of the astronomical tide at Kornwerderzand were obtained from Flater (1998). The surge was calculated from the ECMWF data by applying a simple surge model (van den Brink *et al.*, 2004: equation (1)) to the nearby location of Harlingen (see Figure 1).

Figure 5 shows a Gumbel plot of the time period of non-sluicing, both for the current sea level and for the situation with a sea level rise of 0.25 m. This value is within the expected range of 5–32 cm in 2050 (Houghton *et al.*, 2001), and is the estimate of the medium scenario for the Netherlands (Kors *et al.*, 2000). Apparently, for the present-day sea level a 1 week period of non-sluicing occurs every 25 years. With constant water management practice, a 0.25 m sea level rise would increase the length of the extreme duration of non-sluicing by at least a factor of two. A rise of 0.45 m (which is the extreme scenario for the Netherlands in 2050; Kors *et al.*, 2000) would cause an increase by a factor of three.

4.3. Storm surge barrier closure. The ‘Maeslantkering’ is a storm surge barrier in the ‘Nieuwe Waterweg’ Rhine outlet near Hoek van Holland (see Figure 1), which automatically closes when the water level L_R at Rotterdam is expected to exceed a level of 3 m above MSL. The water level at Rotterdam is determined not only by the Rhine discharge, but also by the tidal motions of the sea and the surges.

The water level at Rotterdam L_R is related statistically to the sea level at Hoek van Holland L_{HvH} and the Rhine discharge at Lobith Q by

$$L_R = L_{HvH} + aQ + bQ^2 \quad (5)$$

where a and b are constants. The average closure frequency of the Maeslantkering is not exactly known, as there has been some debate whether the extreme surges and discharges can be treated independently in the risk analysis.

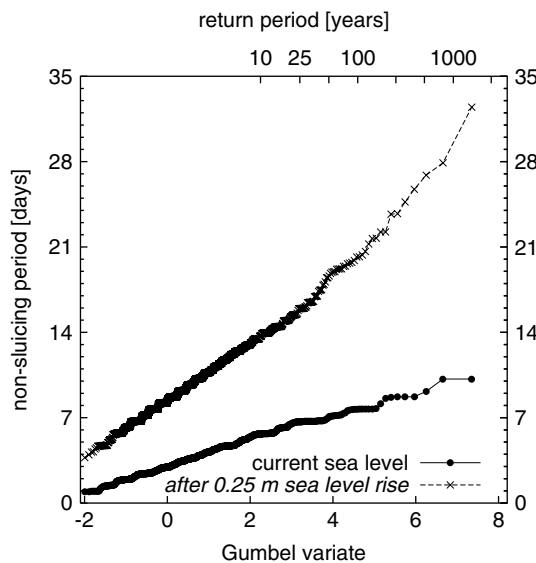


Figure 5. Gumbel plot of the period that surges prevent sluicing from the IJsselmeer into the North Sea, both for current MSL and for the situation after a sea level rise of 25 cm, expected for 2050

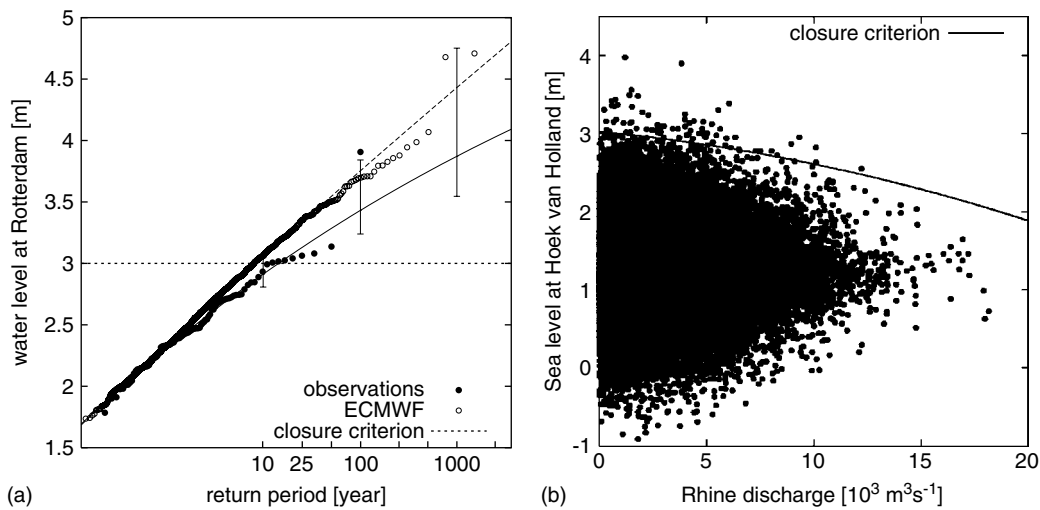


Figure 6. (a) Gumbel plot of the water level with respect to MSL L_R at Rotterdam, both for the observational set and for the ECMWF set. Also shown are the closure criterion, the GEV fits, and the 95% uncertainty intervals for return periods of 10, 100 and 1000 years for the observational set. The closure criterion of the Maeslantkering, $L_R = 3$ m, is indicated. (b) Scatter plot of the water level at Hoek van Holland L_{HvH} versus the Rhine discharge Q for all high-tide values of L_R of the ECMWF set, together with the closure criterion $L_R = 3$ m. According to our analysis, the closure criterion is exceeded once every 8.1 years

We calculated the Rhine discharge according to Equation (4) and the high-tide sea level at Hoek van Holland by calculating the high tide surge every 12 h from the ECMWF data according to van den Brink *et al.* (2004: equation (1)), and adding that value to the astronomical high tide that occurred in the preceding 12 h. A Gumbel plot of L_R is shown in Figure 6(a), both for the observations and for the ECMWF data. The scatter plot of the Rhine discharge and the sea level at Hoek van Holland for the annual maxima of L_R , as well as the closure criterion $L_R = 3$ m, are shown in Figure 6(b). According to the ECMWF data, the criterion is exceeded, on average, once in 8.1 years. Note that most of these events occur because of an extreme surge level rather than an extreme river discharge, due to the small sensitivity of the criterion (Equation (5)) to the river discharge. Note also that no positive correlation is apparent between surges and discharges.

Figure 7 shows that the number of closure events increases exponentially with sea level rise. In this calculation, no greenhouse effect on the tides, surges and Rhine discharges is taken into account. With an increase in the number of closings the average duration of closing will also increase.

4.4. Wave and sea level interaction. The ‘Pettemer zeekering’ is a small stretch of sea dike that closes a gap in the natural coast protection formed by sand dunes near Petten. The design height of the dikes is determined not only by sea level elevations, but also by wave heights, because of run-up of waves. Extreme surges and sea wave heights are correlated, as they both tend to occur during strong northwesterly winds. Failure of the ‘Pettemer zeekering’ may occur if the dike load exceeds the design load (e.g. de Haan and de Ronde, 1998):

$$\text{dike load (m)} \equiv L_P + 0.3H > 7.6 \quad (6)$$

with L_P the sea level at Petten and H the wave height. For the evaluation of Equation (6) we consider the tidal station IJmuiden, located about 30 km south of Petten (Figure 1), for which wave data are also available. The surge was calculated from the ECMWF data by applying the surge model (van den Brink *et al.*, 2004: equation (1)) to Petten/IJmuiden, and then transformed into sea level by adding the astronomical high tides.

The ECMWF data include deep-water wave heights, calculated by the WAM model (Komen *et al.*, 1994). We scaled the ECMWF deep-water wave height to the depth-limited wave height using the following relation

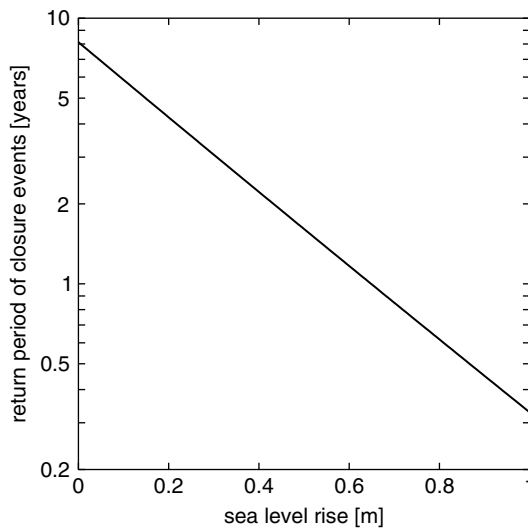


Figure 7. Effect of sea level rise on the frequency of closing the ‘Maeslantkering’. The vertical scale is logarithmic

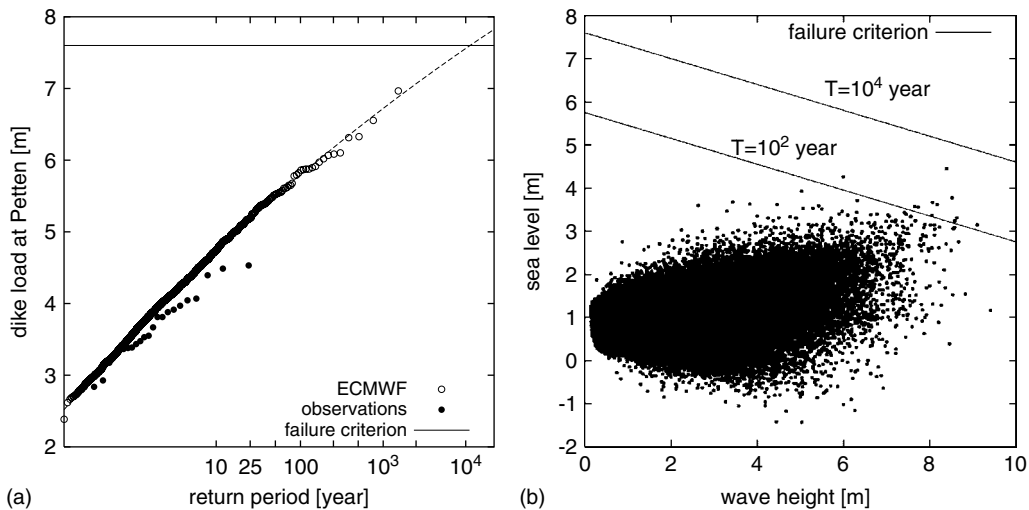


Figure 8. (a) Gumbel plot of the dike load $L_P + 0.3H$ of the Pettemer zeeuwering, with L_P the sea level and H the wave height at Petten, for the ECMWF set (1569 years) and for the observational set (1979–2001). Also shown is the GEV fit to the ECMWF data. The failure level (7.6 m) is indicated by a horizontal line. (b) Scatter plot of L_P versus H for all high-tide events in the ECMWF set. The failure area is reached with a return period of 1×10^4 years. Also shown is the line with a return period of 100 years

(based on Bouws *et al.* (1998), by taking the limit of fully developed wind waves):

$$H_{\text{shallow}} = H_{\text{deep}} \tanh \left[0.63 \left(\frac{h}{H_{\text{deep}}} \right)^{0.75} \right] \tag{7}$$

with H_{shallow} the depth-limited wave height, H_{deep} the ECMWF deep-water wave height and h the water depth (25 m for IJmuiden).

A Gumbel plot of the dike load $L_P + 0.3H$ is shown in Figure 8(a), both for the observations and for the ECMWF data. The scatter plot of the wave height against sea level, as well as the failure criterion at

Petten, is shown in Figure 8(b). The estimate of the exceedance of the failure criterion is 1×10^4 years, i.e. in agreement with the design return period for coastal protection.

5. DISCUSSION AND CONCLUSIONS

The ECMWF seasonal forecast ensembles provide a large dataset that reproduces well the annual extremes of wind over the North Sea and of precipitation over the Rhine basin. This opens the possibility to estimate the return values with return periods up to 10^3 years, semi-empirically which is an order larger than what is possible from the observational sets, and to improve the accuracy of extrapolations to the 10^4 -year level.

Four applications are shown, all of them associated with hydraulic response to synoptic-scale meteorologic events. Checking the results with the extreme-value analysis for observations shows good agreement for surges, waves, precipitation rates and Rhine discharge. This strengthens the belief that the ECMWF data can be considered as a realistic 'climate series' of extended length that is representative for the current climate on a synoptic scale. This opens the possibility to study the extreme far tail from the climatological probability density function, a region that is of great importance for society but whose characteristics cannot be studied from observational records other than by huge extrapolation. The four applications show improved return-value estimates. Two of the applications explore the correlation between violent events of different types.

The type of analysis explored here may be extended to other meteorological elements, such as temperature. However, the application has its limitations. Some of the largest weather-related impacts on society are caused by synoptic-scale systems, but if meso-scale systems (order 10–100 km) are the driving force behind the events, then the ECMWF set cannot represent them. Obvious examples are extreme showers and gusts. Another limitation of the present approach is the use of simple downscaling relations, e.g. the representations for the drag relation in the surge equation, the Rhine discharge (Equation (4)) and the bottom effects in waves (Equation (7)). In principle, these downscaling relations can be improved by using advanced models (e.g. van Deursen and Kwadijk, 1993; Gerritsen *et al.*, 1995).

Despite the encouraging results of our analysis, the estimates of the extreme return values may have a limited validity. As the climate system for present-day conditions may exhibit low-frequency variability, this 17 year dataset may not be entirely representative for the full spectrum of the present-day climate. In fact, the simulations only represent the extreme statistics associated to the single realization of the 1987–2004 period, where the simulations are initiated from.

In order to explore the extreme statistics of the climate in a wider time window, or for different climate conditions than the 1987–2004 window, one has to return to long simulations with climate models, but these lack the benefits mentioned in section 1. A better alternative is to base the analysis on the seasonal prediction hindcasts, as recently produced for the 1958–2001 window in the 'Demeter' project (Palmer *et al.*, 2004).

It is fortunate that ECMWF archived these seasonal forecasts so carefully that a large dataset is available now for an application that was not initially envisioned. As the length of the dataset will only be expanded in the future (with 20 years every month), it will allow for more accurate extreme-value estimations under more general climatological circumstances than the present 1987–2004 baseline.

REFERENCES

- Anderson DLT, Stockdale T, Balmaseda MA, Ferranti L, Vitart F, Doblus-Reyas P, Hagedorn R, Jung T, Vidard A, Troccoli A, Palmer T. 2003. Comparison of the ECMWF seasonal forecast systems 1 and 2, including the relative performance for the 1997/8 El Niño. Technical Report Technical Memoranda 404 ECMWF Shinfield Park, Reading, UK.
- Bouws E, Draper L, Shearman EDR, Laing AK, Feit D, Mass W, Eide LI, Francis P, Carter DJT, Battjes JA. 1998. *Guide to Wave Analysis and Forecasting*, second edition. WMO – No. 702. World Meteorological Organization.
- Buishand TA. 1991. Extreme rainfall estimation by combining data from several sites. *Hydrological Sciences Journal* **36**: 345–365.
- Coles S. 2001. *An Introduction to Statistical Modelling of Extreme Values*. Springer-Verlag: London.
- De Haan L. 1976. Sample extremes: an elementary introduction. *Statistica Neerlandica* **30**: 161–172.
- De Haan L. 1990. Fighting the arch-enemy with mathematics. *Statistica Neerlandica* **44**: 45–68.
- De Haan L, de Ronde J. 1998. Sea and wind: multivariate extremes at work. *Extremes* **1**: 7–45.
- Fink A, Ulbrich U, Engel H. 1996. Aspects of the January 1995 flood in Germany. *Weather* **51**: 34–39.
- Flater D. 1998. Xtide: harmonic tide clock and tide predictor. <http://www.flaterco.com/xtide/> [Last accessed May 2004].

- Gerritsen H, de Vries H, Philippart M. 1995. The Dutch continental shelf model. In *Quantitative Skill Assessment for Coastal Ocean Models*, Lynch D, Davies A (eds). *Coastal and Estuarine Studies*, volume 47. American Geophysical Union.
- Gregory D, Morcrette JJ, Jakob C, Beljaars ACM, Stockdale T. 2000. Revision of convection, radiation and cloud schemes in the ECMWF integrated forecasting system. *Quarterly Journal of the Royal Meteorological Society* **126**: 1685–1710.
- Houghton JT, Ding Y, Griggs DJ, Noguer M, van der Linden PJ, Dai X, Maskell K, Johnson CA (eds). 2001. *Climate Change: The Scientific Basis*. (eds) Cambridge University Press.
- Katz RW, Parlange MB, Naveau P. 2002. Statistics of extremes in hydrology. *Advances in Water Resources* **25**: 1287–1304.
- Komen GJ, Cavaleri L, Donelan M, Hasselmann K, Hasselmann S, Janssen PAEM. 1994. *Dynamics and Modelling Ocean Waves*, volume 1. Cambridge University Press.
- Kors AG, Claessen FAM, Wesseling JW, Können GP. 2000. Scenario's externe krachten voor WB21. In *Waterbeleid voor de 21e eeuw, Advies van de Commissie Waterbeheer 21e eeuw*, Tielrooij F, van Dijk J, de Blécourt-Maas J, van den Ende A, Oosterbaan GA, Overbeek HJ (eds). Technical Report (in Dutch).
- Palmer TN, Alessandri A, Andersen U, Cantelaube P, Davey M, Décluse P, Déque M, Diez E, Doblas-Reyes FJ, Feddersen H, Graham R, Gualdi S, Guérémy J-F, Hagedorn R, Hoshen M, Keenlyside N, Latif M, Lazar A, Maisonnave E, Marletto V, Morse AP, Orfila B, Rogel P, Terres J-M, Thomson MC. 2004. Development of a European multi-model ensemble system for seasonal to inter-annual prediction (DEMETER). *Bulletin of the American Meteorological Society* **85**: 853–872. DOI:10.1175/BAMS-85-6-853
- Palutikof JP, Brabson BB, Lister DH, Adcock ST. 1999. A review of methods to calculate extreme wind speeds. *Meteorological Applications* **6**: 119–132.
- Peilbesluit wateren IJsselmeergebied. 1992. Ministerie van Verkeer en Waterstaat, directoraat-generaal Rijkswaterstaat, directie Flevoland (in Dutch).
- Ritchie H, Temperton C, Simmons AJ, Hortal M, Davies T, Dent D, Hamrud M. 1995. Implementation of the semi-Lagrangian method in a high resolution version of the ECMWF forecast model. *Monthly Weather Review* **123**: 489–514.
- Van den Brink HW, Können GP, Opsteegh JD, van Oldenborgh GJ, Burgers G. 2004. Improving 10⁴-year surge level estimates using data of the ECMWF seasonal prediction system. *Geophysical Research Letters* **31**: L17210.
- Van Deursen WPA, Kwadijk J. 1993. RHINEFLOW: an integrated GIS water balance model for the river Rhine. In *Application of Geographic Information Systems in Hydrology and Water Resources Management*, Kovar K, Nachtnebel HP (eds). *IAHS Publication No. 211*. IAHS Press: Wallingford; 507–519.
- Wolff J-O, Maier-Reimer E, Legutke S. 1997. The Hamburg ocean primitive equation model HOPE. Technical Report No. 13, Deutsches Klimarechenzentrum, Hamburg, Germany.